Title: Agnostic fungi: plant functional types and tissue stoichiometry explain nutrient transfer in common arbuscular mycorrhizal networks of temperate grasslands

Authors: Hilary Rose Dawson[1,2*], Katherine L. Shek[1,2,3], Toby M. Maxwell[1,4], Paul B. Reed[1,2,5], Barbara Bomfim[1,6], Scott D. Bridgham[1,2], Brendan J. M. Bohannan[1,2], Lucas C.R. Silva[1,2,7*]

Affiliations:

1. Institute of Ecology and Evolution, University of Oregon, Eugene, OR 97403 USA
2. Department of Biology, University of Oregon, Eugene, OR 97403 USA
3. Department of Natural Resources and the Environment, University of New Hampshire, Durham NH 03824
4. Department of Biological Sciences, Boise State University, Boise, Idaho, 83725 USA
5. Institute for Applied Ecology, Corvallis, OR 97333 USA
6. Climate and Ecosystem Sciences Division, Lawrence Berkeley National Laboratory, Berkeley, CA 94720 USA
7. Environmental Studies Program, University of Oregon, Eugene, OR 97403 USA

Corresponding authors: H.R.D. hilaryd@uoregon.edu L.C.R.S. lsilva7@uoregon.edu

ORCIDs:

H.R.D.: 0000-0003-4613-762X

K.L.S.: 0000-0001-5629-5782

T.M.M.: 0000-0001-5171-0705

P.B.R.: 0000-0001-7143-7515

B.B.: 0000-0001-9510-2496

S.D.B.: 0000-0003-0614-2678

B.J.M.B.: 0000-0003-2907-1016

L.C.R.S.: 0000-0002-4838-327X

Abstract:

Plants and mycorrhizal fungi form mutualistic relationships that affect how resources flow between organisms and within ecosystems. Common mycorrhizal networks (CMNs) could facilitate preferential transfer of carbon and limiting nutrients but this remains difficult to predict. Do CMNs favor fungal resource acquisition at the expense of plant resource demands (a fungi-centric view), or are they passive channels through which plants regulate resource fluxes (a plant-centric view)? We used stable isotope tracers ($^{13}CO_2$ and $^{15}NH_3$), plant traits, and mycorrhizal DNA to quantify above- and belowground carbon and nitrogen transfer between 18 plant species along a 520-km latitudinal gradient in the Pacific Northwest, USA. Plant functional type and tissue stoichiometry were the most important predictors of interspecific resource transfer. Of "donor" plants, 98% were ^{13}C-enriched, but we detected transfer in only 2% of "receiver" plants. However, all donors were ^{15}N-enriched and we detected transfer in 81% of receivers. Nitrogen was preferentially transferred to annuals (0.26 ± 0.50 mg N per g leaf mass) compared to perennials (0.13 ± 0.30 mg N per g leaf mass). This corresponded with tissue stoichiometry differences. Our findings point to a simple mechanistic answer for long-standing questions regarding transfer of resources between plants via mycorrhizal networks.

Keywords: arbuscular mycorrhizal fungi, carbon, common mycorrhizal networks, ecological stoichiometry, grasslands, nitrogen, plant functional type

Introduction:

Plant-mycorrhizal associations are thought to have emerged as rudimentary root systems over 400 million years ago, facilitating the expansion of terrestrial life that followed[1]. The transformative power of early fungal symbioses is still evident today in all major plant lineages, from bryophytes to angiosperms [2]. Over 85% of all contemporary flowering plant species form symbioses with fungi, with arbuscular mycorrhizal (AM) associations being the most common [3]. Today, the relationships between plants and AM fungi dominates both managed and unmanaged landscapes and are estimated to be responsible for up to 80% of global primary productivity [2]. Fungi are gregarious and form symbioses with more than one individual plant [4]. By extension, it has been widely hypothesized that the multi-plant-fungal relationships form "common mycorrhizal networks" (CMNs) which facilitate carbon and nutrient transfer between organisms, beyond the immediate plant-fungus mutualism formed by individuals. This relationship is often simplified to the mutual exchange of carbon-based photosynthates for limiting soil nutrients that are more readily bioavailable to fungi [5], but is known to exist along a continuum from parasitic to mutualistic [6–9]. A synthesis of empirical research at macro- and micro-levels of ecological organization reveals a gap in understanding of structural and functional properties that could predict how carbon and nutrients are transferred between plants through fungi in CMNs [10].

The literature holds myriad and often complimentary, but sometimes contradictory, hypotheses that could explain the CMN mutualism as a key structural and functional component of ecosystems. For example, the "economics" hypothesis [11] proposes that plants and fungi engage in "trades" of nutrients mined by fungi in exchange for plant photosynthates [12–14]. In the economics hypothesis, the terms of trade between plant and fungi are mediated by supply and

demand for limiting resources, which could create a dynamic market emerging from interactions between environmental, biochemical, and biophysical variables. The “Wood Wide Web” hypothesis emerged from the analysis of isotopically labeled carbon transferred between plants, presumably through fungal mycorrhizae. Simard et al. [15] concluded that plants that allocate carbon to sustain common fungal symbionts also benefit from shared nutrients, while plants associating with mycorrhizal fungi outside that network cannot. Complementing the economic analogy, the “kinship” hypothesis proposes that plants of the same species preferentially receive more resources in CMNs [16,17].

The past two decades have seen extensive but inconclusive research on these hypotheses and how they relate to empirical measurements of CMN structure and function. On the one hand, economic analogies suggest that the reciprocally regulated exchange of resources between plants and fungi in CMNs should favor the most beneficial cooperative partnerships [11,12]. On the other hand, reciprocal transfer is only found in a subset of symbionts under specific conditions, while increased competition in CMNs is a more common observation [18,19]. At the core of this controversy is whether CMNs actively support fungal resource acquisition at the expense of plant resource demands (i.e., a fungi-centric view) or function as passive channels through which plants regulate resource fluxes (i.e., a plant-centric view). If plant-centric, we expect to find that the structure and functioning of CMNs give rise to consistent spatiotemporal patterns of resource allocation akin to those predicted by the kinship hypothesis. If fungi-centric, we expect to find that spatiotemporal patterns of resource allocation reflect the composition and functioning of the fungal community regardless of the connecting plant nodes in CMNs. Data exist to support both opposing views [see 10,20]; therefore, we posit that CMNs are neither plant- nor fungi-centric. Instead, perhaps rather than gregarious, AM fungi are “agnostic” with respect to plant species

96 composition and relatedness, and yet affected by major plant functional traits that are known to
97 influence resource use and allocation. There is no clear evidence to suggest that AM
98 fungi exhibit specificity for plant species as do host-specific pathogens [21]. Even in the systems
99 dominated by ectomycorrhizal (EM) associations where most previous research into CMN
100 structure and function was developed, fungi tend to be generalists, although plant taxa-specific
101 EM fungi occur at relatively high proportion, especially in early successional temperate plant
102 communities [22,23]. Building on previous research, our hypothesis represents a first-principles
103 simplification in which gradients in resource limitation, rather than species-specific plant-fungi
104 interactions, might allow us to better understand and predict the rates and direction of resource
105 transfer in CMNs.

106 To test the "agnostic fungi" hypothesis, we asked if interactions among biophysical and
107 biogeochemical processes could explain resource transfer in CMNs with more accuracy than
108 previous plant- or fungi-centric analogies. We studied how soil resource-use efficiency and plant
109 traits that are known to regulate physiological performance [24] and that are expected to affect
110 the transfer of carbon and nitrogen [25] in paired experiments including restored prairie and
111 pasture experimental sites under ambient conditions and rain exclusion shelters (designed to
112 affect soil water and nutrient mass flow). To test this, we applied ^{15}N-enriched NH3 to plant
113 leaves, which are known to uptake ammonia [26,27], and sampled surrounding plants to examine
114 the transfer of nitrogen using the tracer. Although gases are not the primary source of nitrogen
115 for most plants, applying gaseous nitrogen allowed us to limit the amount leaked into the soil
116 compared to applying nitrogen directly to the soil [28]. We replicated our paired experimental
117 setting at three different locations, with study sites distributed across a 520 km latitudinal
118 gradient. Due to the climatically driven differences in communities across sites, not all species

119 were present at all sites (Table S1); however, all functional groups were present at all sites and
120 most species were present at more than one site. In this experiment, we also sequenced strain-
121 level variation in root fungal DNA, plant functional types, and leaf stoichiometric traits to test if
122 relatedness (same or different species as the donor) explained difference in resource transfer.
123 This allowed us to generalize our inferences about the structure and function of arbuscular
124 CMNs in temperate grasslands. The diversity of plant growth forms included in our study also
125 affect CMN composition and function. For example, Davison et al. [29] found plant growth form
126 altered AM fungal community and functional diversity. Plant total biomass can also increase
127 nitrogen received through a CMN, an effect that may be compounded by whether plants are
128 woody or herbaceous [30]. This could be explained by larger or denser plants providing more
129 carbon. Both plants and fungi have economic spectra characterized by fast or slow traits and
130 nutrient strategies which together form an interacting continuum potentially driven by N
131 availability [31]. It is unclear to what extent plant or fungi characteristics drive these plant-fungal
132 interactions. Therefore, we designed an experiment to quantify how plant-fungal interactions
133 influence the structure and functioning of CMNs across broad environmental gradients and
134 resource constraints.
135
136 **Materials and Methods:**
137 We conducted our experiment at three sites situated on a 520 km latitudinal transect that
138 spans three Mediterranean climates: cool, moist (northern site; Tenino, WA) to warm, moist
139 (central site; Eugene, OR) to warm, dry (southern site; Selma, OR). Each circular plot was 3 m in
140 diameter. Half of our plots were restored prairie systems (n = 10 per site) while the other half of
141 the plots had introduced pasture grasses established prior to restoration (n = 10 per site).

142 Restored prairie plots were mowed, raked, received herbicide, and seeded in 2014-2015,
143 followed by seeding in fall 2015, 2016, and 2017 [32]. We erected rainout shelters that excluded
144 40% of the rainfall on half the plots at each site (n = 10 rain exclusion, 10 control per site; Fig.
145 1).

146 All plants in our system have the potential to form associations with AM fungi (Table S1)
147 [33–35]. Previous work demonstrated that the rainout shelters had minimal effects on
148 aboveground community structure or function [24], possibly due to the shoulder season effect of
149 the Mediterranean rain seasonality. This network of experimental sites was established in 2010
150 and has been extensively studied since then [32,36–39] including work on mycorrhizal fungi
151 [40,41]. Treatments had marginal effects on the soil water potential (especially during the early
152 growing season). Pasture plots were dominated by one to a few species of introduced perennial
153 grasses which we targeted as donors in these plots. We used different species of perennial grass
154 at each site. For restored prairie plots, we targeted the native perennial forb *Sidalcea malviflora*
155 ssp. *virgata* common to ambient and drought treatments at all sites. Despite those differences, we
156 did not find significant changes in the average plant community composition or productivity
157 under rain exclusion, which also did not affect morphological and functional traits (e.g., specific
158 leaf area, iWUE, and C:N ratios) of the functional groups we selected for this experiment
159 [24,36].

160 To test our new hypothesis, we built upon those preliminary data with a dual isotope label
161 approach as follows. We labeled perennial plants central to each plot (hereafter, 'donors') and
162 monitored leaf ^{15}N and ^{13}C for the surrounding plants ('receivers') for up to 21 days. In addition,
163 we sampled roots and soils at 21 days post-labelling. We characterized AM fungal DNA isolated
164 from the root samples, as well as stable isotopes in all leaf and root samples. Our experimental

design was nested in a multi-year experiment where data loggers were used to continuously measure temperature and moisture in all the manipulated plots.

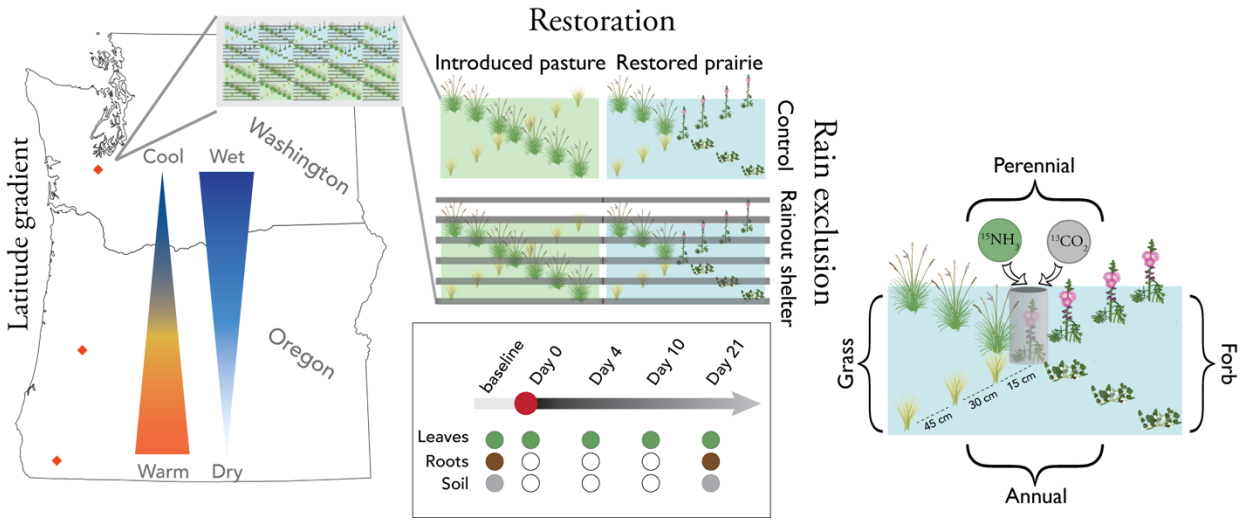

Figure 1. Schema of experimental set up, sampling, and effects of rainout shelters. Figure shows the three location of the sites (orange points on map) in relation to the climatic gradient (cool to warm, wet to dry). Each site has twenty plots which are a full factorial representation of the restoration and rain exclusion treatments. Each plot had a central perennial plant that was labeled with isotopically enriched gas (shown with a grey cylinder here) and we sampled plants of each functional type at three distances from the central labelled plant. Inset shows the temporal sampling scheme of leaves, roots and soil.

Isotopic labelling

At each site, we selected a healthy perennial forb (*Sidalcea malviflora* ssp. *virgata* in restored prairie plots [except in one plot where we used *Eriophyllum lanatum* due to a lack of *S. malviflora ssp. virgata*]), or a perennial grass (*Alopecurus pratensis, Schedonorus arundinaceus,* or *Agrostis capillaris*) in pasture plots at the center of each plot to receive the isotopic labels. On

182 sunny days between 11AM and 3PM at peak productivity for each site, we applied isotopically
183 enriched carbon (^{13}C) and nitrogen (^{15}N) as a pulse of carbon dioxide (CO_2) and ammonia (NH_3)
184 to the leaves of target "donor" species common across experimental sites. We performed the
185 labeling experiment using custom-made field-deployable clear chambers with internal fans built
186 to allow gas mixing and fast in situ assimilation of isotopic labels, following established
187 protocols developed in previous isotopically labeling studies [e.g., 42–44]. Before performing
188 the experiment, we tested our approach in the field to optimize gas exposure and labeling
189 amounts, which included checking for leaks and contamination outside of the chamber. We
190 covered the donor plant with a clear plastic cylindrical chamber and injected gas in sequence at
191 20-minute intervals. For $^{13}CO_2$, we made three injections of 2 mL pure CO_2 (enriched at 98 atm
192 % ^{13}C) to double the amount of CO_2 in the chamber each time. For NH_3, we made two injections
193 of 10 mL pure NH_3 (98 atm% ^{15}N) at 20 minute intervals. The dates of application were based on
194 peak productivity estimated from Normalized Different Vegetation Index (NDVI) at each site
195 [see 32 for details]. We sampled leaves from each donor plant immediately after labeling (time
196 point 0) as well as from all plants approximately 4 days (time point 1), 10 days (time point 2),
197 and 21 days (time point 3) post-labelling as logistics permitted (Fig. 1, Table S2). We also
198 collected leaves at time points 1, 2, and 3 from up to twelve plants in each plot representing three
199 replicates of factorial grass/forb structural groups and annual/perennial life history strategies
200 (Table S1). The number of plants and represented groups depended on which plants were
201 growing in each plot. For example, pasture plots were limited to only grasses and the northern
202 pasture plots had only perennial grasses.
203 By applying enriched gases only to the aboveground portions of established perennial
204 donor plants, we introduced the isotopic tracer to both the plant and mycorrhizal fungal tissues

with minimal exposure of the soil to the tracers. At the end of the experiment, we harvested entire plants and the soil surrounding the roots at time point 3 and kept them in cool conditions until processing. We separated the roots and rhizospheres, and collected roots from each plant, selecting approximately ten ~3 cm fine root fragments per sample (i.e., third order or finer, where available) for DNA extraction and identification. All roots and rhizosphere soils were stored at -80º C until processing.

Baseline and Resource Transfer Calculations

Before isotopic labeling, we collected soil, leaves, and roots from each site. We collected soils in late spring and early summer 2019 to 20 cm depth in each plot. From these soil samples, we removed root fragments that represented the typical roots seen in each plot. We collected leaves for each species in each plot; however, these leaves were contaminated with ^{15}N during transport. To replace contaminated samples, we separately sampled leaves from biomass samplings collected in late spring and early summer 2019, ensuring that annual and perennial grasses and forbs were represented at each site.

We oven-dried all samples at 65º C to constant mass and encapsulated them for stable isotope analysis. All stable isotope analysis was done at UC Davis Stable Isotope Facilities using an Elementar Vario EL Cube or Micro Cube elemental analyzer (Elementar Analysensysteme GmbH, Hanau, Germany) interfaced to a PDZ Europa 20-20 isotope ratio mass spectrometer (Sercon Ltd., Cheshire, UK). We calculated the amount of carbon and nitrogen in each plant compartment (leaves and roots) using standard label recovery equations [44], using baseline values measured before application of the labelled gases to capture background variations in isotopic composition of unenriched leaves, roots, and soil samples.

We designated all samples with greater than two standard deviations above baseline samples as “enriched” in a particular isotope. Baseline values were calculated on a site by rain exclusion treatment basis by plant functional type basis (Table S3). We calculated these values for each plant functional type because our sampling scheme was designed around these functional types. Site-specific baseline soil and root isotope ratios represent the whole community because of interconnected rhizospheres where is it was not possible to identify

specific species. In all cases, baseline values fell within the expected range for our region (Fig. 2). For each enriched sample, we calculated isotope excess as

Equation 1

$$atm\%_{excess} = atm\%_{post\ label} - atm\%_{baseline}$$

For enriched donor plants, we calculated % derived from label immediately following label application as

Equation 2

$$\%DFL_{donor} = \frac{atm\%_{excess}}{atm\%_{labelling\ gas} - atm\%_{baseline}} * 100$$

For enriched receiver plants, we calculated % derived from label (%NDFL and %CDFL, respectively) for each relevant point in space and time as [40]

Equation 3

$$\%DFL_{receiver} = \frac{atm\%_{receiver\ excess}}{atm\%_{\ donor\ excess}} * 100$$

When we calculated %DFL in roots, we used donor leaves as the source (atm% donor excess). We then calculated the amount derived from label on a per mass basis as

Equation 4

$$DFL\ (\text{mg N / g leaf}) = 1000 * 1g * \left(\frac{N\ or\ C\%}{100}\right) * \left(\frac{DFL\%}{100}\right)$$

We calculated intrinsic water-use efficiency following Farquhar and Richards [45] using the baseline ^{13}C values from the original samples because the contamination only occurred with ^{15}N. Because of sampling discrepancies, we did not have intrinsic water-use efficiency data for 32 plants.

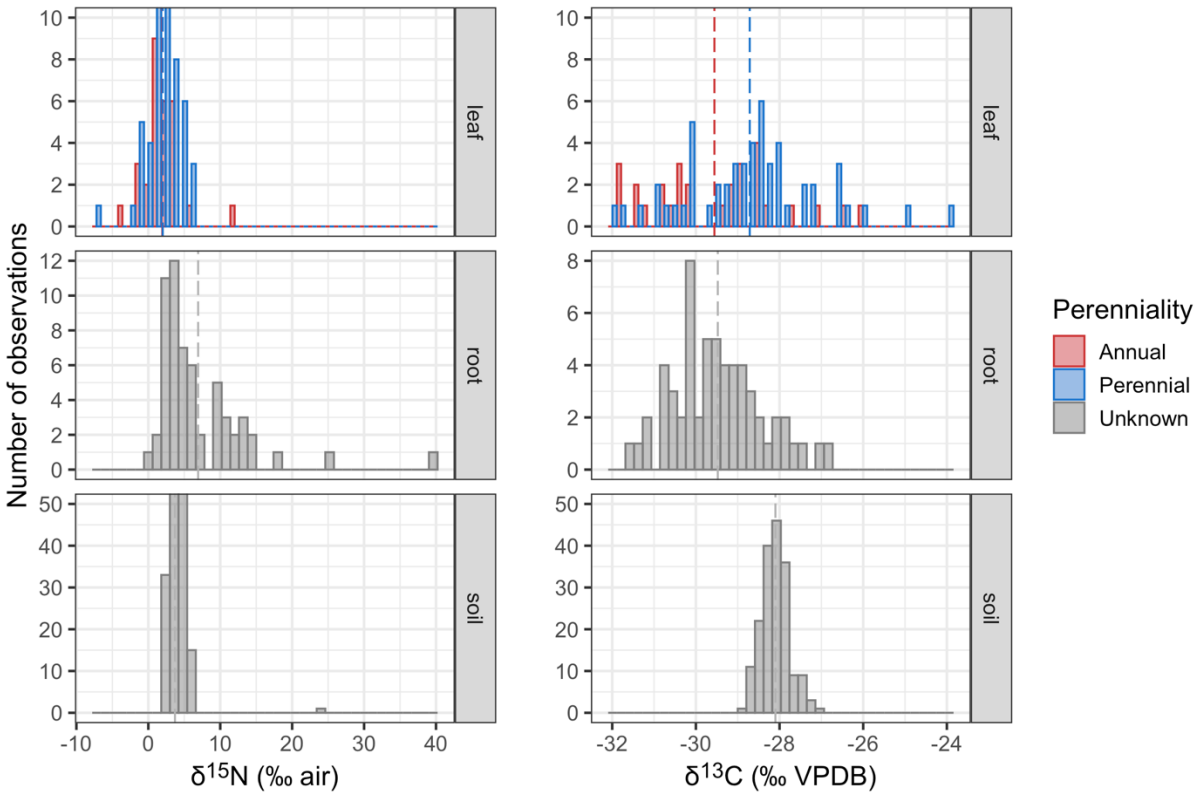

Figure 2. Natural abundance of stable isotopes in leaves, roots, and soil before labelling. Dashed lines indicate mean value. Exact values used to calculate derivation from label (Eq. 1 – Eq. 4) are available in Table S3.

To better understand post-labelling soil enrichment, we selected a subset of rhizosphere soils that represented six donor plants at each site divided equally between restored prairie and pasture plots, and selected the three most highly ^{15}N-enriched interspecific receivers in each plot across the sites. In addition, we sampled three most highly enriched interspecific receivers at each site and restored prairie-introduced pasture combination (if they had not been sampled previously). Because pasture plots were sometimes monodominant grasses, we sampled the top three enriched intraspecific receivers at each site and treatment. In total, this came to 48 post-labelling soil samples in 29 plots.

267 *Fungal DNA analysis*

268 We extracted DNA from roots of 450 plants harvested at time point 3 (21 days post-label)
269 using Qiagen DNeasy Powersoil HTP kits (Qiagen, Hilden, Germany). We only analyzed DNA
270 from roots, not from the soils collected from each plant's rhizosphere. We characterized each
271 sample's AM fungal composition with a two-step PCR protocol that amplified a ~550bp
272 fragment of the SSU rRNA gene (the most well-supported region for AM fungal taxonomic
273 resolution [46]. We used WANDA (5'- CAGCCGCGGTAATTCCAGCT- 3') and AML2 (5'-
274 GAACCCAAACACTTTGGTTTCC-3') primers [47,48]. We used primers with unique indices
275 so we could multiplex several projects on a single run. We quantified successful PCR amplicons
276 with the Quant-iT PicoGreen dsDNA Assay Kit (Invitrogen, Waltham, MA, USA) on a
277 SpectraMax M5E Microplate Reader (Molecular Devices, San Jose, CA, USA) before purifying
278 with QIAquick PCR Purification kits (Qiagen). We sequenced the purified pools on the Illumina
279 MiSeq platform (paired-end 300bp, Illumina Inc., San Diego, CA, USA) at the University of
280 Oregon Genomics and Cell Characterization Core Facility (Eugene, OR, USA). Reads were
281 deduplicated with UMI-tools using unique molecular identifiers (UMIs) inserted during PCR
282 [49].

283 We assigned amplicon sequence variants (ASVs) using the dada2 pipeline (version
284 1.18.0) with standard quality filtering and denoising parameters [50]. The dada2 pipeline
285 maintains strain-level diversity at the scale of individual sequence variants rather than clustering
286 sequences into OTUs. This fine-scale measure of fungal sequence diversity was particularly
287 important for our analyses to maintain the greatest chance of detecting a single AM fungal
288 'individual' in multiple plant root samples. Taxonomy was assigned to ASVs using the
289 MaarjAM database (2019 release) [51]. We used a Bayesian mixture model in the DESeq2

290 package [52] to scale ASV counts within and across samples to avoid artificial taxon abundance
291 biases [53].
292
293 *Data analysis*
294 We performed all analyses in R ver. 4.0.4 [54]. We removed one outlier plant with a ^{15}N
295 atm% more than twice as high as the next highest measurement. We also removed five
296 mislabeled samples. To meet statistical assumptions, we only included data from enriched plants
297 with successful root fungal DNA extraction in our analyses and figures. We limited receivers to
298 those for which we also had sufficient root fungal DNA. In total, from 1440 leaves measured for
299 isotopic content and with successfully recovered fungal DNA, we analyzed data from 391 unique
300 plants: 53 donors and 338 receivers.
301 We tested the relationship between receiver leaf %DFL and plant traits (grass/forb,
302 annual/perennial, iWUE, C:N, degrees of connectivity, interaction term between grass/forb and
303 annual/perennial) and site conditions (position on latitude gradient, pasture/restored, rain
304 exclusion treatment, distance from donor, time from labelling) with a mixed-effect ANOVA
305 (plot as random effect; Table 1). We constructed a phyloseq object using the ASV table with
306 normalized counts[55], and used iGraph, metagMisc, and RCy3 [56–58] to create networks for
307 each plot. In each network, nodes represented individual plants and edges between nodes
308 represent plants sharing at least one fungal DNA sequence variant. The weighted edges are based
309 on how many fungal ASVs were shared among plants. We calculated degrees of connectivity
310 with tidygraph [59] to examine how many plants each individual plant was 'connected' to (by
311 means of shared fungal ASVs) in each plot (Fig. 3). We also calculated whether each receiver
312 plant shared fungal ASVs with the central donor plant in each plot. We visualized individual plot

networks in CytoScape. We visualized shifts in AM fungal community composition using non-metric multi-dimensional scaling (NMDS) in the vegan package, demonstrating the AM fungal community similarity across plants [60].

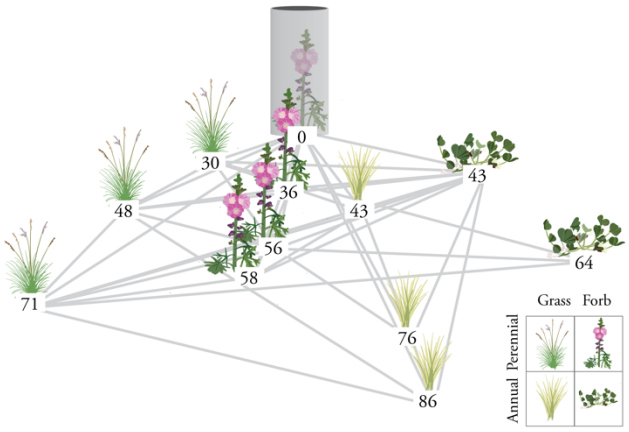

Figure 3. Example of how networks were constructed for each plot. The grey cylinder indicates the donor plant for the plot. Numbers beneath the receivers are the distance (in centimeters) from the donor. Degrees were calculated as how many plants each individual plant was connected to by shared fungal ASVs; for example, the perennial grass at 71 cm has 7 degrees.

Results:

All donors were ^{15}N-enriched in their leaves at time of labelling. Two donors were not ^{13}C-enriched in their leaves at time of labelling. We recovered DNA data from the roots of 88.3% of donors. We sampled 1,444 leaves from 434 receiver plants at three time points. Of these leaves, 81.0% were ^{15}N-enriched and 2.4% were ^{13}C-enriched. We recovered DNA from the roots of 77.9% of the receivers. At time point 3 (roughly 21 days post-labelling), we collected roots from 46 of the initial 60 donors and 306 of the initial 434 receivers. Of the roots of the collected donors, 97.8% were still 15N-enriched and 23.9% were still ^{13}C-enriched at time

point 3. Of the roots of the collected receivers, 33.0% were still ^{15}N-enriched and 10.5% were still ^{13}C-enriched at time point 3.

Assimilation of isotopic tracers was similar between labeled "donor" plants with no significant differences on average between sites or experimental treatments within sites, including rainfall exclusion or restored status (Fig. S1). At all sites, foliar assimilation of ^{15}N and ^{13}C by donor plants led to enrichment levels ranging from approximately 5-10 fold higher than baselines. Foliar enrichment levels decreased consistently at all sites and treatments over the 21 day sampling period. Annual forbs had the greatest enrichment level and perennial forbs the lowest enrichment level (Fig. 4). We found significant spatial and temporal differences in foliar and root isotope ratios in donors and receivers resulting from interspecific transfer of carbon and nitrogen (Fig. S2; Table 1). Receiver foliar enrichment levels did not correlate with donor foliar enrichment levels within the same plot (Fig. S3).

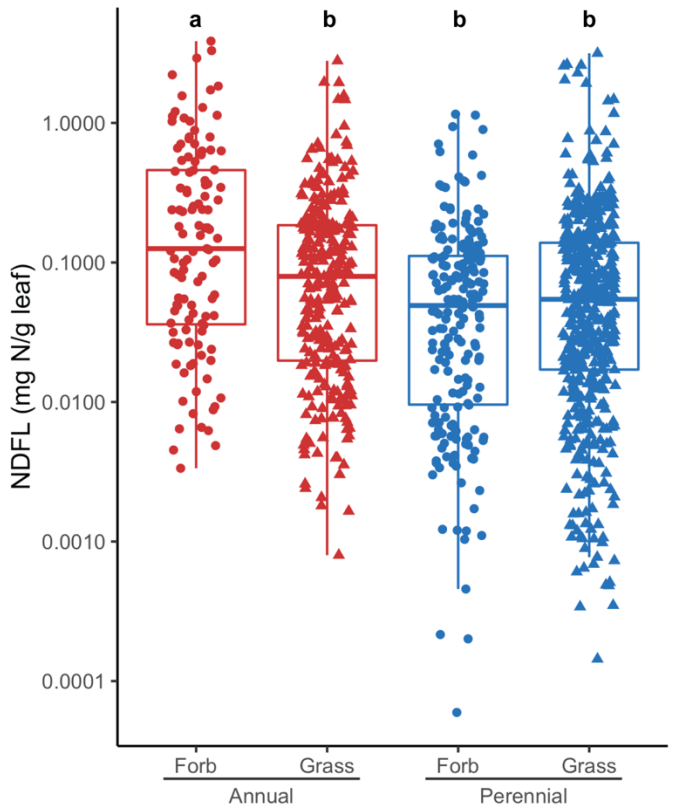

343

344 **Figure 4. Annuals had greater leaf nitrogen derived from label (NDFL) scaled by mass**

345 **than perennials.** Points represent enriched individual receiver plants with associated DNA data

346 at one time point of sampling. All three post-enrichment time points are shown. Y-axis is log10

347 scale. See Fig. S2 for values over distance and Fig. S4 for NDFL in roots as well as CDFL in

348 roots and leaves.

349

350

351 **Table 1. ANOVA results effects on leaf nitrogen derived from label (%NDFL).** Only
352 enriched receiver leaves with associated DNA data were included in the analysis (n = 1094).
353 Leaf %CDFL results available in Table S4.

	DF	χ^2	P-value
Fixed effects			
Annual/perennial	**1**	**10.33**	**<0.001**
Grass/forb	**1**	**11.45**	**<0.001**
Same species as donor	1	0.54	0.463
Degree of connectivity	1	0.17	0.68
iWUE	1	0.06	0.81
C:N	**1**	**36.78**	**<0.001**
Site	2	0.69	0.71
Drought treatment	1	0.51	0.48
Restoration treatment	1	0.91	0.34
Distance from donor	**1**	**9.72**	**0.002**
Time from labelling	**1**	**84.05**	**<0.001**
Annual/perennial: Grass/forb interaction	**1**	**7.87**	**0.01**
Random effect			
Plot			**<0.001**

354

355 Allocation of ^{13}C and ^{15}N tracers to roots and subsequent transfer to "receiver" species
356 did not follow expected patterns (e.g., despite donors being perennial, annual receivers were
357 more enriched, indicating that relatedness did not drive the transfer, Fig. 4, Table 1). Allocation
358 and transfer varied significantly between functional groups due to their intrinsic differences in
359 tissue stoichiometry (Table 1). We selected 18 common annual/perennial and grass/forb species

of receiver plants, which revealed significant differences between functional types for NDFL (Fig. 4) but little detectable CDFL relative to baseline (Fig. S2). Rain exclusion treatment, restoration treatment, and site did not affect interspecific transfer of nitrogen (Fig. S5; ANOVA, $P > 0.05$, Table 1). We observed very low carbon enrichment, but of the 2.4% of leaves that were enriched in carbon, plant functional type and site affected carbon transfer (Table S4). We did, however, observe significant differences in nitrogen transfer by plant functional type (Table 1), mirroring intrinsic differences in tissue stoichiometry and iWUE (Fig. 5), despite no significant enrichment in soils collected from the rhizosphere of those same plants (Fig. S6). We also found that C:N affected NDFL, although not in a simple linear manner and with no apparent correlation between NDFL and iWUE (Fig. 5). We did detect a low level of soil enrichment in 1 out of 30 receiver soil samples (0.377 atm% ^{15}N) and 5 out of 18 donor soil samples (ranging from 0.376 to 0.479 atm% ^{15}N; Fig. S6).

Annuals had greater ^{15}N foliar enrichment compared to perennials (ANOVA, $P < 0.001$, Tables 1 and 2). Foliar enrichment decreased over both time and space (ANOVA $P < 0.001$; Fig. S1, Fig. S2). On average, annuals had a lower leaf nitrogen content and higher C:N than perennials (Table 2, Fig. 5). Forbs had higher NDFL than grasses (ANOVA, $P < 0.001$, Table 1) as well as a lower C:N. There was a significant interaction between annual/perennial and grass/forb form (ANOVA, $P = 0.003$, Table 1). There was no correlation between the relatedness of donors and receivers in 15N-enrichment (table 1).

380 **Table 2. Leaf nitrogen derived from label (NDFL) and leaf tissue nitrogen (N%) four days**

381 **after labeling.**

			%NDFL				**NDFL (mg N/g leaf)**				**N (%)**			
		n	*Mean*	*SD*	*Min*	*Max*	*Mean*	*SD*	*Min*	*Max*	*Mean*	*SD*	*Min*	*Max*
Annual	**Forb**	54	6.528	9.769	0.101	56.005	0.749	0.819	0.041	3.858	0.749	0.819	0.041	3.858
	Grass	92	4.847	9.032	0.098	63.884	0.34	0.463	0.011	2.79	0.340	0.463	0.011	2.790
Perennial	**Forb**	67	0.952	1.069	0.090	5.582	0.214	0.228	0.021	1.156	0.214	0.228	0.021	1.156
	Grass	148	1.632	3.066	0.088	22.434	0.252	0.484	0.013	2.948	0.252	0.484	0.013	2.948

382

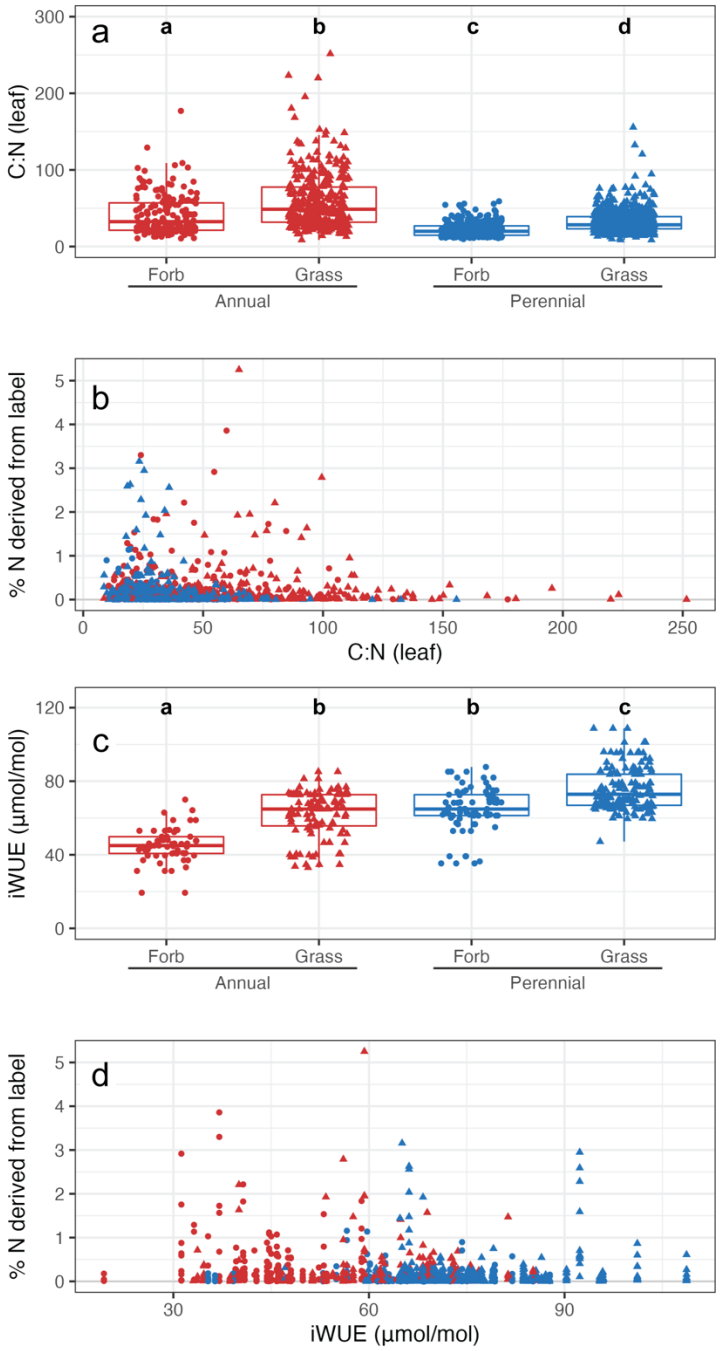

383

384 **Figure 5. Stoichiometric and functional traits compared to nitrogen derived from transfer.**

385 A) Leaf C:N by annual/perennial. B) Percent ^{15}N derived from label (DFL) compared to C:N in

386 leaves. C) iWUE by annual/perennial as measured before labelling. D) Percent ^{15}NDFL

compared to iWUE in leaves at all time points. Letters above boxplots indicate significant differences.

Our analysis of fungal community composition shows a high degree of connectivity between plants of different species but no obvious pattern of connectedness that could explain preferential nutrient transfer by plant functional groups. We found that 97.25% ± 8.01 (SD) of all plant roots within each experimental plot shared at least one fungal DNA sequence variant (ASV) with another plant of the same plot. Fungal community composition was similar across plant functional groups (Fig. 6, PERMANOVA pseudo-F statistic = 2.269, $R^2 = 0.005$, p = 0.001). Annual plants shared fungi with more plants in the same plot (4.74 plants ± 2.62 SD) compared to perennials (4.04 plants ± 2.49 SD ; t-test, P = 0.019; Table S5), but degrees of connectivity did not predict nitrogen transfer (Table 1). Seventy-three percent of plants were colonized by four or fewer fungi and shared fungi with five or fewer other plants in the plot, making it difficult to determine if strength of connectivity altered nitrogen transfer (Fig. S7).

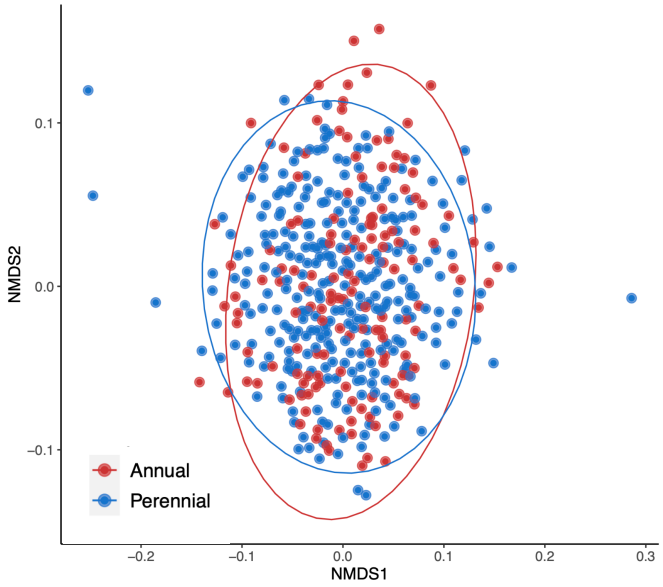

Figure 6. NMDS of fungal communities. Each point represents an individual plant ordinated by the Bray Curtis dissimilarities for AM fungal composition. PERMANOVA pseudo-F statistic = 2.269, $R^2 = 0.005$, $p = 0.001$.

Discussion:

In our extensively replicated spatiotemporal isotopic tracer experiment, the assimilation and allocation of limiting resources in CMNs was neither plant- nor fungi-centric. Our data show that AM fungi are "agnostic" with respect to plant species composition and relatedness, and that the transfer of nitrogen (an important nutrient that can limit plant growth in our system) is regulated by major functional traits that are known to influence resource use and allocation in plant communities. The rates and direction of resource transfer in CMNs, inferred from pulse labeling and recovery of ^{15}N in leaves and rhizospheres, can be predicted from leaf C:N and distance from donor species (Table 1). Across all sites and treatments, we observed a stronger sink for ^{15}N in annual plants (Table 2), indicating preferential transfer of limiting resources to

418 that functional group of plants. We applied the 15N enriched label to perennial species in all
419 plots, so this greater enrichment in annual plants precludes a preference for receiver plants of the
420 same species as would be expected under the kinship hypothesis (Table 1). Although plants
421 shared ~97% fungal ASVs in their roots (Fig. 6), connectivity did not predict ^{15}N transfer (Table
422 1), and thus we found no evidence for a fungi-centric hypothesis based on which all connected
423 plants would have been expected to be equally enriched in ^{15}N. Our data suggest that rates and
424 direction of resource transfer in CMNs reflect plant nutrient requirements and spatial proximity.
425 We designed this experiment to be informed by previous hypotheses on how carbon and
426 nitrogen transfer occurs in highly connected CMNs, where a dilution of the applied ^{13}C label is
427 to be expected given the vast amounts of carbon in the soil and plant biomass. We conducted
428 repeated spatiotemporal sampling of isotopic-enrichment levels at increasing distances from
429 donor species, days to weeks after labelling, and in well-established communities exposed to
430 multiple years of experimental treatments, expecting to find evidence of kinship (i.e., greatest
431 resource transfer in plants of the same species), driven by CMN economics (i.e., ^{15}N transfer
432 rates coinciding with ^{13}C investment in root and fungal mass). Our donor plants were perennials
433 while annuals received, on average, an order of magnitude higher enrichment. Thus, we
434 discarded kinship as a possible driver of transfer in this system. We also did not find evidence of
435 a relationship between ^{15}N in leaves and ^{13}C in roots because we did detect ^{15}N-enrichment in
436 leaves but no ^{13}C-enrichment in roots. We did, however, find significant ^{13}C-enrichment in the
437 donor plants. Therefore, our data do not support either hypothesis, and instead suggest AM fungi
438 are "agnostic" with respect to plant species partnerships, forming CMNs where the rates and
439 direction of resource transfer ultimately reflects a sink-source strength effect, consistent with

440 previous observations of stoichiometric source-sink manipulations of carbon and nitrogen within
441 plants [61–63], but in our case observed at the community scale.

442 Nitrogen enrichment levels remained high in leaves and many roots at the end of the
443 experiment, allowing us to measure NDFL across the community and infer the main drivers of N
444 transfer. However, carbon enrichment levels faded before plants were harvested approximately
445 21 days post-labelling, either due to losses via respiration or redistribution in CMNs where it
446 became undetectable in all but a few cases. After controlling for variation in assimilation rates by
447 calculating NDFL, we found that annual plants received greater ^{15}N-enrichment than perennial
448 plants. Plants closest to the donor were most enriched, and ^{15}N-enrichment decreased over time
449 (Fig. S2, Fig. S3). Plant level of connectivity through an assumed CMN did not predict ^{15}N-
450 enrichment. Although the rainout shelters had limited effect, there were major differences across
451 the latitudinal gradient represented by the sites in temperature and soil moisture availability
452 [24,32]; however, neither treatment nor site affected our results.

453 The major drivers of differences in allocation of ^{13}C and ^{15}N to roots and subsequent
454 transfer to "receiver" species were the intrinsic difference in plant functional types and correlated
455 traits, including measured leaf C:N. Previous studies in northern California under environmental
456 conditions similar to those found in our southernmost experimental site showed rapid (days to
457 weeks) transfer of ^{15}N applied to the leaves of ectomycorrhizal pines to surrounding annual AM
458 plant receivers [64]. Those results were interpreted as evidence for agnostic CMNs because
459 "direct fungal connections are not necessary for N transfer among plants" and "leaves of the
460 annual plants had greater ^{15}N derived from source and were more enriched (^{15}N at % excess and
461 δ^{15}N values) than perennial receivers, irrespective of the mycorrhizal type." Similarly, as
462 proposed by He et al. [64], our observation of agnostic ^{15}N transfer from donor to receivers

463 suggests that annual plants were a strong sink for N which could be explained by stoichiometric
464 gradients that affect root exudation and recapture of N-containing materials from rhizodeposition
465 [65,66]. Although our study included two species with symbiotic N fixation ability could have
466 altered some of the baseline data but even if a plot was fully dominated by legumes that
467 difference would represent a minor effect relative to the pulse label application. Our data
468 corroborate rapid agnostic transfer among AM plants, with no detectable enrichment in root or
469 soil ^{13}C near roots 21 days post-labelling, but do not allow us to determine general mechanisms
470 that are responsible for the ^{15}N transfers.

471 We inferred a high connectivity between plants within each given treatment and site
472 given the highly similar fungal composition in the root systems of both perennial and annual
473 plants (Fig. 6). Given the constraints of ASV-identified data, we did this analysis on a strain-
474 level scale and it is possible that separate spores of the same ASV separately infected plants
475 within the same plot. However, we are reasonably confident in our use of fungal ASVs as a
476 proxy for connectivity given the strong overlap in our community and because individuals of one
477 ASV can anastomose in the soil [67]. This overlap could explain the lack of support for the
478 kinship hypothesis in our dataset and offers further support for stoichiometric gradients in
479 general, and C:N gradients in particular, as a principal control of terms of trade in CMNs
480 [11]. Because we observed such high rates of shared ASVs (~97%) and we observed high levels
481 of N-enrichment in receivers at our first post-label sampling point four days after application, we
482 could not test whether receivers connected to donors or whether plants were connected to the
483 network affected ^{15}N transfer. We found unexpectedly low soil isotopic-enrichment (fig. S6)
484 which suggested that the labels did not remain in the fungal network. This low level was likely
485 driven by the fact that we did not sample soils until 21 days after labeling and hyphal turnover

for grass-associated AM fungi can be less than one month [68]. Because N is a major limiting nutrient in this system, according to the current paradigm of CMNs, it would be quickly taken up and recycled or transferred rather than accumulating in the soil.

We found that plant-soil stoichiometric gradients and functional traits were the strongest drivers of resource sharing in grassland CMNs. We interpret this finding as evidence of biochemical and biophysical sinks, in which nutrients are allocated to plants with the greatest need for those nutrients, either through a 'passive' mycorrhizal network or direct uptake from soil, or that nutrients should be allocated through water flow. Expanding on previous studies, we propose that agnostic AM fungi facilitate spatiotemporal dynamics of carbon and nitrogen transfer through CMNs in ways that are neither plant- nor fungi-centric. That is, plants and fungi that are located closer together in space and with stronger demand for resources over time are more likely to receive larger amounts of those limiting resources.

Acknowledgements:

The authors thank the Siskiyou Field Institute, The Nature Conservancy, and Capitol Land Trust for providing sites for this experiment, Laurel Pfeifer-Meister, Bitty Roy, Bart Johnson, Graham Bailes, Aaron Nelson, and Matthew Krna for their contributions to experimental design, Emily Scherer for her assistance with sample analysis, Bitty Roy, Leonel Sternberg, Timothy A. Doane, and five anonymous reviewers for comments on the manuscript, and numerous others for assistance with the HOPS project. This experiment was funded by National Science Foundation Macrosystems Biology grant #1340847, Plant Biotic Interactions grant #1758947, and Convergence Accelerator Pilot grant #1939511.

Competing interests:

The authors have no competing interests to declare.

Author contributions:

L.C.R.S, S.D.B., and B.J.M.B. designed the research; H.R.D., K.L.S., T.M.M., B.B., and P.B.R. performed the research; H.R.D. led the data analysis and manuscript preparation with K.L.S. assisting; all authors contributed to revising the manuscript and approved the publication.

Data availability:

Data used in these analyses will be available online at the Data Dryad repository (https://doi.org/10.5061/dryad.7pvmcvdxt) after publication.

References:

1. Kenrick P, Strullu-Derrien C. 2014 The Origin and Early Evolution of Roots 1. *Plant Physiol* , 570–580. (doi:10.1104/pp.114.244517)
2. van der Heijden MGA, Martin FM, Selosse MA, Sanders IR. 2015 Mycorrhizal ecology and evolution: the past, the present, and the future. *New Phytologist* **205**, 1406–1423. (doi:10.1111/NPH.13288)
3. Brundrett MC. 2009 Mycorrhizal associations and other means of nutrition of vascular plants: understanding the global diversity of host plants by resolving conflicting information and developing reliable means of diagnosis. *Plant Soil* **320**, 37–77. (doi:10.1007/s11104-008-9877-9)
4. Selosse MA, Richard F, He X, Simard SW. 2006 Mycorrhizal networks: des liaisons dangereuses? *Trends Ecol Evol*. **21**, 621–628. (doi:10.1016/j.tree.2006.07.003)
5. Smith SE, Read DJ (David J). 2008 *Mycorrhizal symbiosis*. Academic Press.
6. Mariotte P, Meugnier C, Johnson D, Thébault A, Spiegelberger T, Buttler A. 2013 Arbuscular mycorrhizal fungi reduce the differences in competitiveness between dominant and subordinate plant species. *Mycorrhiza* **23**, 267–277. (doi:10.1007/S00572-012-0465-8/FIGURES/4)
7. Klironomos JN. 2003 Variation in plant response to native and exotic arbuscular mycorrhizal fungi. *Ecology* **84**, 2292–2301. (doi:10.1890/02-0413)
8. Johnson NC, Graham JH, Smith FA. 1997 Functioning of mycorrhizal associations along the mutualism–parasitism continuum. *New Phytologist* **135**, 575–585. (doi:10.1046/J.1469-8137.1997.00729.X)

9. Luo X, Liu Y, Li S, He X. 2023 Interplant carbon and nitrogen transfers mediated by common arbuscular mycorrhizal networks: beneficial pathways for system functionality. *Front Plant Sci* **14**. (doi:10.3389/fpls.2023.1169310)

10. Silva LCR, Lambers H. 2021 Soil-plant-atmosphere interactions: structure, function, and predictive scaling for climate change mitigation. *Plant Soil* , 1–23. (doi:10.1007/s11104-020-04427-1)

11. Kiers ET *et al.* 2011 Reciprocal rewards stabilize cooperation in the mycorrhizal symbiosis. *Science (1979)* **333**, 880–882. (doi:10.1126/science.1208473)

12. Fellbaum CR, Mensah JA, Cloos AJ, Strahan GE, Pfeffer PE, Kiers ET, Bücking H. 2014 Fungal nutrient allocation in common mycorrhizal networks is regulated by the carbon source strength of individual host plants. *New Phytologist* **203**, 646–656. (doi:10.1111/nph.12827)

13. Werner C, Dubbert M. 2016 Resolving rapid dynamics of soil-plant-atmosphere interactions. *New Phytologist* **210**, 767–769. (doi:10.1111/nph.13936)

14. Averill C, Bhatnagar JM, Dietze MC, Pearse WD, Kivlin SN. 2019 Global imprint of mycorrhizal fungi on whole-plant nutrient economics. *Proc Natl Acad Sci U S A* **116**, 23163–23168. (doi:10.1073/PNAS.1906655116/SUPPL_FILE/PNAS.1906655116.SD01.CSV)

15. Simard SW, Perry DA, Jones MD, Myrold DD, Durall DM, Molina R. 1997 Net transfer of carbon between ectomycorrhizal tree species in the field. *Nature* **388**, 579–582. (doi:10.1038/41557)

16. Tedersoo L, Bahram M, Zobel M. 2020 How mycorrhizal associations drive plant population and community biology. *Science (1979)* **367**.

(doi:10.1126/SCIENCE.ABA1223/ASSET/64588F4D-CCDD-4041-891C-3C19CD9AEDF9/ASSETS/GRAPHIC/367_ABA1223_F3.JPEG)

17. Pickles BJ, Wilhelm R, Asay AK, Hahn AS, Simard SW, Mohn WW. 2017 Transfer of ^{13}C between paired Douglas-fir seedlings reveals plant kinship effects and uptake of exudates by ectomycorrhizas. *New Phytologist* **214**, 400–411. (doi:10.1111/nph.14325)

18. Walder F, van der Heijden MGA. 2015 Regulation of resource exchange in the arbuscular mycorrhizal symbiosis. *Nat Plants* **1**. (doi:10.1038/nplants.2015.159)

19. Weremijewicz J, Sternberg L da SLO, Janos DP. 2016 Common mycorrhizal networks amplify competition by preferential mineral nutrient allocation to large host plants. *New Phytologist* **212**, 461–471. (doi:10.1111/nph.14041)

20. Figueiredo AF, Boy J, Guggenberger G. 2021 Common Mycorrhizae Network: A Review of the Theories and Mechanisms Behind Underground Interactions. *Frontiers in Fungal Biology* **0**, 48. (doi:10.3389/FFUNB.2021.735299)

21. Lee E-H, Eo J-K, Ka K-H, Eom A-H. 2013 Mycobiology diversity of arbuscular mycorrhizal fungi and their roles in ecosystems. **41**, 121–125. (doi:10.5941/MYCO.2013.41.3.121)

22. Spencer MW, Roy BA, Thornton TE, Silva LCR, McGuire KL. 2023 Logging has legacy effects on the structure of soil fungal communities several decades after cessation in Western Cascade forest stands. *Frontiers in Forests and Global Change* **6**, 41. (doi:10.3389/FFGC.2023.791766)

23. McMahen K, Guichon SHA, Anglin CD, Lavkulich LM, Grayston SJ, Simard SW. 2022 Soil microbial legacies influence plant survival and growth in mine reclamation. *Ecol Evol* **12**, e9473. (doi:10.1002/ECE3.9473)

24. Dawson HR, Maxwell TM, Reed PB, Bridgham SD, Silva LCR. 2022 Leaf traits predict water-use efficiency in U.S. Pacific Northwest grasslands under rain exclusion treatment. *J Geophys Res Biogeosci* **127**, e2022JG007060. (doi:10.1029/2022JG007060)

25. Peaucelle M *et al.* 2019 Covariations between plant functional traits emerge from constraining parameterization of a terrestrial biosphere model. *Global Ecology and Biogeography* **28**, 1351–1365. (doi:10.1111/GEB.12937)

26. Farquhar GD, Firth PM, Wetselaar R, Weir B. 1980 On the Gaseous Exchange of Ammonia between Leaves and the Environment: Determination of the Ammonia Compensation Point. *Plant Physiol* **66**, 710–714. (doi:10.1104/pp.66.4.710)

27. Sutton MA, Erisman JW, Dentener F, Möller D. 2008 Ammonia in the environment: From ancient times to the present. *Environmental Pollution* **156**, 583–604. (doi:10.1016/j.envpol.2008.03.013)

28. Silva LCR, Salamanca-Jimenez A, Doane TA, Horwath WR. 2015 Carbon dioxide level and form of soil nitrogen regulate assimilation of atmospheric ammonia in young trees. *Sci Rep* **5**, 13141. (doi:10.1038/srep13141)

29. Davison J *et al.* 2020 Plant functional groups associate with distinct arbuscular mycorrhizal fungal communities. *New Phytologist* **226**, 1117–1128. (doi:10.1111/nph.16423)

30. He Y, Cornelissen JHC, Wang P, Dong M, Ou J. 2019 Nitrogen transfer from one plant to another depends on plant biomass production between conspecific and heterospecific species via a common arbuscular mycorrhizal network. *Environmental Science and Pollution Research* **26**, 8828–8837. (doi:10.1007/S11356-019-04385-X/FIGURES/4)

31. Ward EB, Duguid MC, Kuebbing SE, Lendemer JC, Bradford MA. 2022 The functional role of ericoid mycorrhizal plants and fungi on carbon and nitrogen dynamics in forests. *New Phytologist* (doi:10.1111/NPH.18307)

32. Reed PB *et al.* 2019 Prairie plant phenology driven more by temperature than moisture in climate manipulations across a latitudinal gradient in the Pacific Northwest, USA. *Ecol Evol* **9**, 3637–3650. (doi:10.1002/ece3.4995)

33. Soudzilovskaia NA *et al.* 2020 FungalRoot: global online database of plant mycorrhizal associations. *New Phytologist* **227**, 955–966. (doi:10.1111/nph.16569)

34. Chaudhary VB *et al.* 2016 Data Descriptor: MycoDB, a global database of plant response to mycorrhizal fungi. *Nature* , 3:160028. (doi:10.1038/sdata.2016.28)

35. Dickie IA, Martínez-García LB, Koele N, Grelet GA, Tylianakis JM, Peltzer DA, Richardson SJ. 2013 Mycorrhizas and mycorrhizal fungal communities throughout ecosystem development. *Plant Soil* **367**, 11–39. (doi:10.1007/s11104-013-1609-0)

36. Reed PB, Pfeifer-Meister LE, Roy BA, Johnson BR, Bailes GT, Nelson AA, Bridgham SD. 2021 Introduced annuals mediate climate-driven community change in Mediterranean prairies of the Pacific Northwest, USA. *Divers Distrib* **00**, 1–12. (doi:10.1111/ddi.13426)

37. Reed PB *et al.* 2021 Climate manipulations differentially affect plant population dynamics within versus beyond northern range limits. *Journal of Ecology* **109**, 664–675. (doi:10.1111/1365-2745.13494)

38. Reed PB *et al.* 2021 Climate warming threatens the persistence of a community of disturbance-adapted native annual plants. *Ecology* **102**, e03464. (doi:10.1002/ecy.3464)

39. Peterson ML *et al.* 2020 Latitudinal gradients in population growth do not reflect demographic responses to climate. *Ecological Applications* (doi:10.1002/eap.2242)

634 40. Wilson H, Johnson BR, Bohannan B, Pfeifer-Meister LE, Mueller R, Bridgham SD. 2016
635 Experimental warming decreases arbuscular mycorrhizal fungal colonization in prairie
636 plants along a Mediterranean climate gradient. *PeerJ* **2016**, 1–22.
637 (doi:10.7717/peerj.2083)
638 41. Vandegrift R, Roy BA, Pfeifer-Meister L, Johnson BR, Bridgham SD. 2015 The
639 herbaceous landlord: integrating the effects of symbiont consortia within a single host.
640 *PeerJ* **3**, e1379. (doi:10.7717/peerj.1379)
641 42. Earles JM, Sperling O, Silva LCR, McElrone AJ, Brodersen CR, North MP, Zwieniecki
642 MA. 2016 Bark water uptake promotes localized hydraulic recovery in coastal redwood
643 crown. *Plant Cell Environ* **39**, 320–328. (doi:10.1111/pce.12612)
644 43. Sperling O, Silva LCR, Tixier A, Théroux-Rancourt G, Zwieniecki MA. 2017
645 Temperature gradients assist carbohydrate allocation within trees. *Sci Rep* **7**, 3265.
646 (doi:10.1038/s41598-017-03608-w)
647 44. Silva LCR, Salamanca-Jimenez A, Doane TA, Horwath WR. 2015 Carbon dioxide level
648 and form of soil nitrogen regulate assimilation of atmospheric ammonia in young trees.
649 *Sci Rep* **5**, 13141. (doi:10.1038/srep13141)
650 45. Farquhar GD, Richards RA. 1984 Isotopic Composition of Plant Carbon Correlates With
651 Water-Use Efficiency of Wheat Genotypes. *Functional Plant Biology* **11**, 539–552.
652 46. Dumbrell AJ, Ashton PD, Aziz N, Feng G, Nelson M, Dytham C, Fitter AH, Helgason T.
653 2011 Distinct seasonal assemblages of arbuscular mycorrhizal fungi revealed by
654 massively parallel pyrosequencing. *New Phytologist* **190**, 794–804. (doi:10.1111/J.1469-
655 8137.2010.03636.X)

656 47. Langmead B, Salzberg SL. 2012 Fast gapped-read alignment with Bowtie 2. *Nature*
657 *Methods 2012 9:4* **9**, 357–359. (doi:10.1038/nmeth.1923)
658 48. Lee J, Lee S, Young JPW. 2008 Improved PCR primers for the detection and
659 identification of arbuscular mycorrhizal fungi. *FEMS Microbiol Ecol* **65**, 339–349.
660 (doi:10.1111/J.1574-6941.2008.00531.X)
661 49. Smith T, Heger A, Sudbery I. 2017 UMI-tools: modeling sequencing errors in Unique
662 Molecular Identifiers to improve quantification accuracy. *Genome Res* **27**, 491–499.
663 (doi:10.1101/gr.209601.116)
664 50. Callahan BJ, McMurdie PJ, Rosen MJ, Han AW, Johnson AJA, Holmes SP. 2016
665 DADA2: High-resolution sample inference from Illumina amplicon data. *Nature Methods*
666 *2016 13:7* **13**, 581–583. (doi:10.1038/nmeth.3869)
667 51. Öpik M, Vanatoa A, Vanatoa E, Moora M, Davison J, Kalwij JM, Reier Ü, Zobel M. 2010
668 The online database MaarjAM reveals global and ecosystemic distribution patterns in
669 arbuscular mycorrhizal fungi (Glomeromycota). *New Phytologist* **188**, 223–241.
670 (doi:10.1111/J.1469-8137.2010.03334.X)
671 52. Love MI, Huber W, Anders S. 2014 Moderated estimation of fold change and dispersion
672 for RNA-seq data with DESeq2. *Genome Biol* **15**, 1–21. (doi:10.1186/S13059-014-0550-
673 8/FIGURES/9)
674 53. Anders S, Huber W. 2010 Differential expression analysis for sequence count data.
675 *Genome Biol* **11**, 1–12. (doi:10.1186/GB-2010-11-10-R106/COMMENTS)
676 54. R Core team. 2015 R Core Team. *R: A Language and Environment for Statistical*
677 *Computing. R Foundation for Statistical Computing , Vienna, Austria. ISBN 3-900051-07-*
678 *0, URL http://www.R-project.org/.* **55**, 275–286.

679 55. McMurdie PJ, Holmes S. 2013 phyloseq: An R Package for Reproducible Interactive
680 Analysis and Graphics of Microbiome Census Data. *PLoS One* **8**, e61217.
681 (doi:10.1371/JOURNAL.PONE.0061217)
682 56. Nepusz T, Csardi G. 2006 The igraph software package for complex network research.
683 57. Mikryukov V. 2017 metagMisc. (doi:10.5281/ZENODO.571403)
684 58. Gustavsen JA, Pai S, Isserlin R, Demchak B, Pico AR. 2019 RCy3: Network biology
685 using Cytoscape from within R. *F1000Res* **8**, 1774.
686 (doi:10.12688/F1000RESEARCH.20887.3)
687 59. Petersen T. 2022 tidygraph: A Tidy API for Graph Manipulation.
688 60. Oksanen J *et al.* 2022 vegan: Community Ecology Package.
689 61. Cai Z, Xie T, Xu J. 2021 Source–sink manipulations differentially affect carbon and
690 nitrogen dynamics, fruit metabolites and yield of Sacha Inchi plants. *BMC Plant Biol* **21**,
691 1–14. (doi:10.1186/S12870-021-02931-9/FIGURES/8)
692 62. Ruiz-Vera UM, De Souza AP, Long SP, Ort DR. 2017 The role of sink strength and
693 nitrogen availability in the down-regulation of photosynthetic capacity in field-grown
694 Nicotiana tabacum L. at elevated CO2 concentration. *Front Plant Sci* **8**, 998.
695 (doi:10.3389/FPLS.2017.00998/BIBTEX)
696 63. Tegeder M, Masclaux-Daubresse C. 2018 Source and sink mechanisms of nitrogen
697 transport and use. *New Phytologist* **217**, 35–53. (doi:10.1111/NPH.14876)
698 64. He X, Bledsoe CS, Zasoski RJ, Southworth D, Horwath WR. 2006 Rapid nitrogen transfer
699 from ectomycorrhizal pines to adjacent ectomycorrhizal and arbuscular mycorrhizal plants
700 in a California oak woodland. *New Phytologist* **170**, 143–151. (doi:10.1111/j.1469-
701 8137.2006.01648.x)

65. Mayer J, Buegger F, Jensen ES, Schloter M, Heß J. 2003 Estimating N rhizodeposition of grain legumes using a 15N in situ stem labelling method. *Soil Biol Biochem* **35**, 21–28. (doi:10.1016/S0038-0717(02)00212-2)

66. Høgh-Jensen H, Schjoerring JK. 2001 Rhizodeposition of nitrogen by red clover, white clover and ryegrass leys. *Soil Biol Biochem* **33**, 439–448. (doi:10.1016/S0038-0717(00)00183-8)

67. Mikkelsen BL, Rosendahl S, Jakobsen I. 2008 Underground resource allocation between individual networks of mycorrhizal fungi. *New Phytologist* **180**, 890–898. (doi:10.1111/J.1469-8137.2008.02623.X)

68. See CR, Keller AB, Hobbie SE, Kennedy PG, Weber PK, Pett-Ridge J. 2022 Hyphae move matter and microbes to mineral microsites: Integrating the hyphosphere into conceptual models of soil organic matter stabilization. *Glob Chang Biol* **28**, 2527–2540. (doi:10.1111/gcb.16073)

Supporting information

Table S1. List of species at each site with number of leaf samples per species.

Table S2. Collection dates for each time point at each site.

Table S3. Baseline values used to calculate amount derived from label (DFL).

Table S4. ANOVA results effects on leaf carbon derived from label (%CDFL).

Table S5. List of fungal ASVs by annuals and perennials.

Figure S1. Enrichment decreases over time in labelled plants.

Figure S2. Decreased receiver enrichment with distance from donor in leaves and roots.

Figure S3. Receiver enrichment did not correlate with donor enrichment.

Figure S4: Enrichment derived from label for A) CDFL in leaves, B) NDFL in roots, and C) CDFL in roots.

Figure S5. No trend in ^{15}N-enrichment across site and rain exclusion treatment.

Figure S6. Limited soil enrichment 21 days after labelling.

Figure S7. Histogram of connectivity metrics showing left skew.